Available online at www.sciencedirect.com

ScienceDirect

Ceramics International 40 (2014) 81–86

CERAMICS INTERNATIONAL

www.elsevier.com/locate/ceramint

Electrochemical characteristics of $LiNi_{0.7}Co_{0.3}O_2$ synthesized from different combinations of hydro-oxides, carbonates, and oxides at 800 °C

Myoung Youp Song[a], Ho Rim[b], Hye Ryoung Park[c,*]

[a]Division of Advanced Materials Engineering, Hydrogen & Fuel Cell Research Center, Engineering Research Institute, Chonbuk National University, 567 Baekje-daero Deokjin-gu Jeonju 561-756, Republic of Korea

[b]ASE Korea, 494 Munbal-dong Paju-si Gyeonggi-do 413-790, Republic of Korea

[c]School of Applied Chemical Engineering, Chonnam National University, 77 Yongbong-ro Buk-gu Gwangju 500-757, Republic of Korea

Received 12 April 2013; received in revised form 25 May 2013; accepted 28 May 2013
Available online 2 June 2013

Abstract

Cathode active materials with a composition of $LiNi_{0.7}Co_{0.3}O_2$ were synthesized by solid-state reaction at 800 °C using Li_2CO_3 or $LiOH \cdot H_2O$, NiO or $NiCO_3$, and $CoCO_3$ or Co_3O_4 as sources of Li, Ni, and Co, respectively. The electrochemical properties of the synthesized samples were then investigated. The structures of the synthesized $LiNi_{0.7}Co_{0.3}O_2$ samples were analyzed, and the microstructures of the samples were observed. The curves of voltage vs. x in $Li_xNi_{0.7}Co_{0.3}O_2$ for the first charge-discharge and the intercalated and deintercalated Li quantity Δx were studied. The $LiNi_{0.7}Co_{0.3}O_2$ sample synthesized from $LiOH \cdot H_2O$, NiO, and Co_3O_4 had the largest first discharge capacity of 162 mAh/g with a discharge capacity deterioration rate of 9.1 mAh/g/cycle.

Keywords: $LiNi_{0.7}Co_{0.3}O_2$; Solid-state reaction; Various starting materials; Curve of voltage vs. x in $Li_xNi_{0.7}Co_{0.3}O_2$; Discharge capacity

1. Introduction

Recent rapid developments in portable electronic devices have increased demand for compact and light-weight batteries. Lithium secondary batteries have drawn a great deal of attention as rechargeable batteries, having higher volumetric and gravimetric energy densities than other rechargeable batteries such as nickel–cadmium and nickel-metal hydride batteries. Lithium secondary batteries also have advantages such as lack of a memory effect and slow self-discharge loss. Interest is also growing in lithium secondary batteries for military, electric vehicle, and aerospace applications.

Materials that can intercalate and deintercalate Li ions are transition metal chalcogenides (TiS_2, MoS_2, and $NbSe_3$) and transition metal oxides (MnO_2, V_6O_{13}, $LiCoO_2$, $LiNiO_2$, $LiMnO_2$, and $LiMn_2O_4$).

Transition metal oxides such as $LiCoO_2$ [1–5], $LiNiO_2$ [6–13], and $LiMn_2O_4$ [14–20] have been investigated as cathode materials for lithium secondary batteries [21]. $LiCoO_2$ has large diffusivity and high operating voltage, and can be synthesized relatively easily. However, it contains an expensive element, Co. $LiNiO_2$ has large discharge capacity [22], and is relatively economically and environmentally friendly. However, since Li and Ni are similar in size ($Li^+ = 0.72$ Å and $Ni^{2+} = 0.69$ Å), $LiNiO_2$ is usually obtained in a non-stoichiometric composition, $Li_{1-y}Ni_{1+y}O_2$ [23,24]. The Ni^{2+} ions in the lithium planes obstruct the movements of the Li+ ions during intercalation and deintercalation [5,25].

The drawbacks of $LiCoO_2$ and $LiNiO_2$ may be compensated for by incorporating $LiCoO_2$ and $LiNiO_2$ phases into $LiNi_{1-y}Co_yO_2$ compositions, because the presence of cobalt stabilizes the structure in a strictly two-dimensional fashion, thus facilitating the

*Corresponding author. Tel.: +82 62 530 1885; fax: +82 62 530 1889.
E-mail address: hyrpark@naver.com (H.R. Park).

0272-8842/$ - see front matter © 2013 Elsevier Ltd and Techna Group S.r.l. All rights reserved.
http://dx.doi.org/10.1016/j.ceramint.2013.05.106

reversibility of the intercalation and deintercalation reactions [26–38]. Rougier et al. [26] reported that stabilization of the two-dimensional character of the structure by cobalt substitution in $LiNiO_2$ is correlated with an increase in cell performance, due to the decrease in the amount of extra nickel ions in inter-slab spaces that impede lithium diffusion. $LiMn_2O_4$ contains a relatively inexpensive element, Mn, and is environmentally friendly, but its cycling performance is poor.

Different starting materials have been used to synthesize $LiNi_{1-y}Co_yO_2$ by solid-state reaction [26–30,32–34,38–42]. $LiOH \cdot H_2O$ or Li_2CO_3, NiO or $NiCO_3$, Co_3O_4, and $CoCO_3$ have been used as starting materials [40].

In this work, $LiNi_{0.7}Co_{0.3}O_2$ cathode materials were synthesized by solid-state reaction at 800 °C using Li_2CO_3 or $LiOH \cdot H_2O$, NiO or $NiCO_3$, and $CoCO_3$ or Co_3O_4 as sources of Li, Ni, and Co, respectively. The electrochemical properties of the synthesized samples were examined, the structures of the synthesized $LiNi_{0.7}Co_{0.3}O_2$ samples were analyzed, and the microstructures of the samples were observed. The curves of voltage vs. x in $Li_xNi_{0.7}Co_{0.3}O_2$ for the first charge-discharge and the intercalated and deintercalated Li quantity Δx were also studied.

2. Experimental

Li_2CO_3 or $LiOH \cdot H_2O$, NiO or $NiCO_3$, and $CoCO_3$ or Co_3O_4 were used as starting materials to synthesize $LiNi_{0.7}Co_{0.3}O_2$ by solid-state reaction. All starting materials were purchased from Aldrich Co. and were 99.9% pure.

Fig. 1 schematically illustrates the experimental procedure for the synthesis of $LiNi_{0.7}Co_{0.3}O_2$ using Li_2CO_3 or $LiOH \cdot H_2O$, NiO or $NiCO_3$, and $CoCO_3$ or Co_3O_4 as the sources of Li, Ni, and Co, respectively, and the characterization of the synthesized samples. The starting materials for $LiNi_{0.7}Co_{0.3}O_2$ were sufficiently mixed and pelletized. The pellet was then heat-treated in air at 650 °C for 20 h, ground, mixed, pelletized, and calcined at 800 °C for 20 h. The pellet was cooled at a rate of 50 °C/min, and then ground, mixed, and pelletized again. Finally, it was calcined at 800 °C for 20 h.

Phase identification of the synthesized samples was carried out by X-ray diffraction (XRD) using Cu Kα radiation (Mac-Science Co., Ltd.). The scanning rate was 16°/min, and the scanning range of the diffraction angle (2θ) was $10° \leq 2\theta \leq 70°$. The morphologies of the samples were observed using a scanning electron microscope (SEM).

Electrochemical cells consisted of $LiNi_{0.7}Co_{0.3}O_2$ as a positive electrode, Li foil as a negative electrode, and an electrolyte of 1 M $LiPF_6$ in a 1:1 (volume ratio) mixture of Ethylene Carbonate (EC) and Dimethyl Carbonate (DMC). Whatman glass–fiber was used as the separator. The cells were assembled in an argon-filled dry box. To fabricate the positive electrode, 89 wt% synthesized oxide, 10 wt% acetylene black, and 1 wt% Polytetrafluoroethylene (PTFE) binder were mixed in an agate mortar. By introducing Li metal, Whatman glass-fiber, the positive electrode, and the electrolyte, the cell was assembled. All electrochemical tests were performed at room temperature using a potentiostatic/galvanostatic system (Mac-Pile system, Bio-Logic Co., Ltd.). The cells were cycled at a current density of 200 μA/cm^2 at a voltage range of 3.2–4.3 V.

3. Results and discussion

The XRD patterns of $LiNi_{0.7}Co_{0.3}O_2$ and $LiCoO_2$ powders calcined at 800 °C for 40 h using Li_2CO_3, $NiCO_3$, and $CoCO_3$ as starting materials are shown in Fig. 2. The peaks correspond to those of the $LiNiO_2$ phase, which has α-$NaFeO_2$ structure with a space group of $R\bar{3}m$. The fraction of each phase can be calculated from the intensity ratios of the 003 and 104 peaks since the 003 peak originates from the diffraction of only the $R\bar{3}m$ α-$NaFeO_2$ structure while the 104 peak originates from the diffractions of both the $R\bar{3}m$ α-$NaFeO_2$ and $Fm\bar{3}m$ NaCl structures. The value of the intensity ratio of the 003 and 104

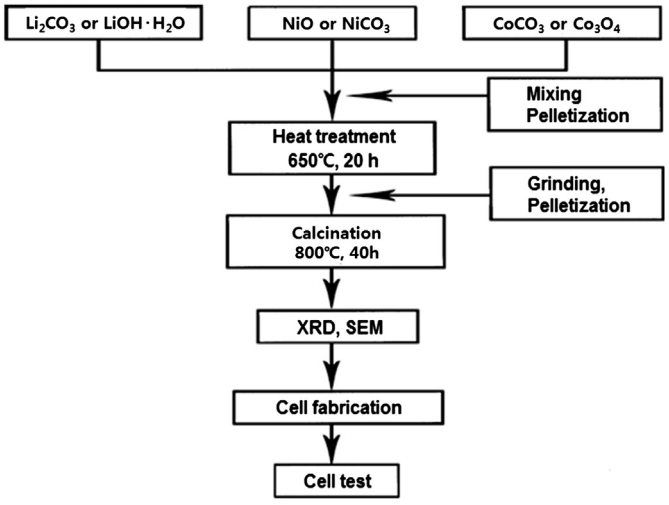

Fig. 1. Experimental procedure for $LiNi_{0.7}Co_{0.3}O_2$ synthesis using Li_2CO_3 or $LiOH \cdot H_2O$, NiO or $NiCO_3$, and $CoCO_3$ or Co_3O_4 as the sources of Li, Ni, and Co, respectively, and characterization of the synthesized $LiNi_{0.7}Co_{0.3}O_2$.

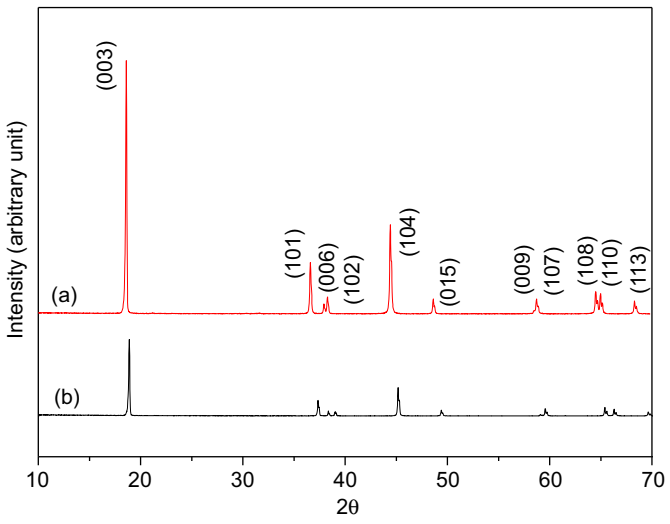

Fig. 2. X-ray (CuKα) diffraction patterns of (a) $LiNi_{0.7}Co_{0.3}O_2$ and (b) $LiCoO_2$ synthesized from Li_2CO_3, $NiCO_3$, and $CoCO_3$.

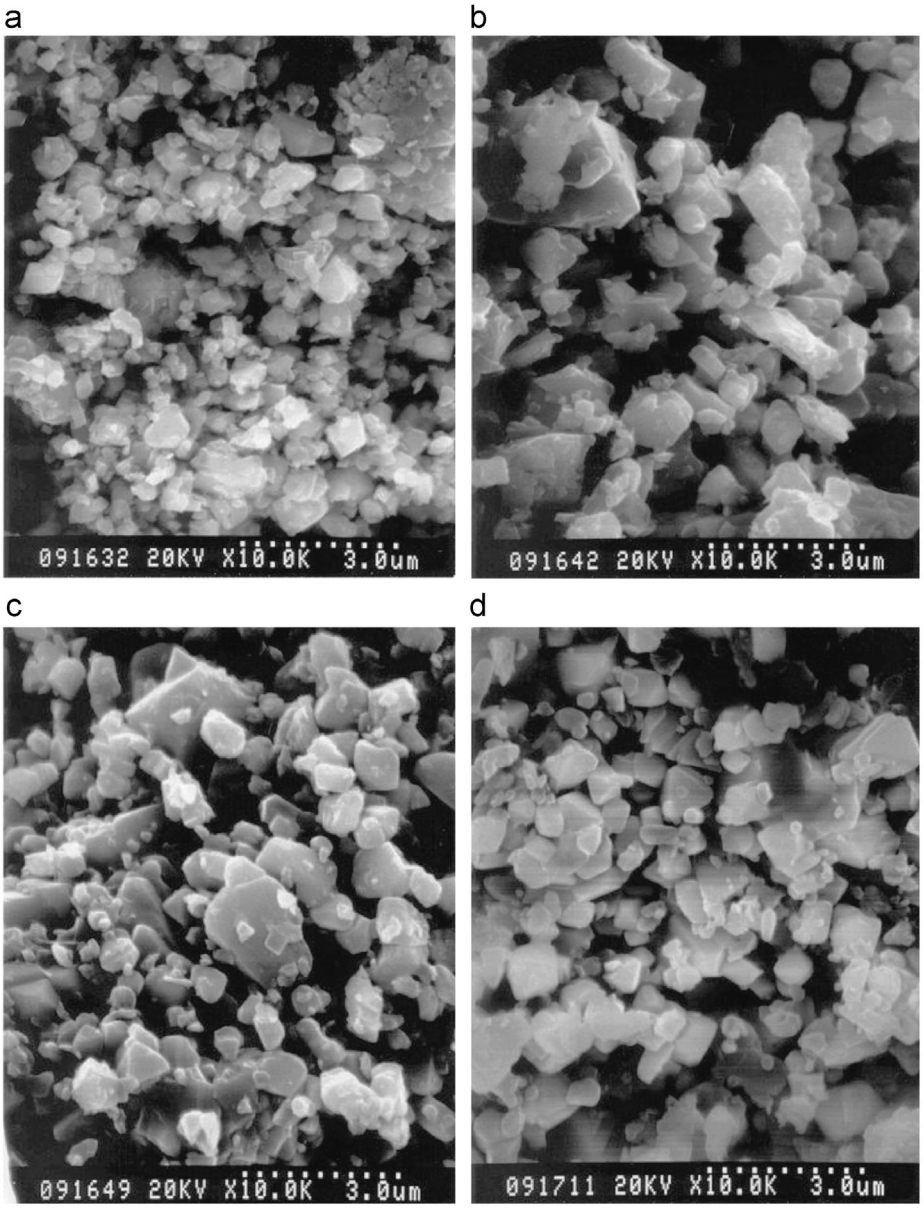

Fig. 3. SEM micrographs of the $LiNi_{0.7}Co_{0.3}O_2$ synthesized at 800 °C using the following combinations of starting materials: (a) Li_2CO_3, NiO, and $CoCO_3$, (b) $LiOH \cdot H_2O$, NiO, and Co_3O_4, (c) Li_2CO_3, NiO, and Co_3O_4, and (d) Li_2CO_3, $NiCO_3$, and $CoCO_3$.

peaks, I_{003}/I_{104}, for a completely stoichiometric composition $LiNiO_2$ was reported to be about 1.3 by Morales et al. [24]. Ohzuku et al. [39] reported that, as the intensity ratio of the 003 and 104 peaks increases, the degree of displacement of the nickel and lithium ions decreases, and also that electroactive $LiNiO_2$ showed a clear split of the (108) and (110) lines, which appear at diffraction angles near $2\theta = 65^o$ in XRD patterns. The XRD pattern of the $LiNi_{0.7}Co_{0.3}O_2$ powder synthesized using $LiCO_3$, $NiCO_3$, and $CoCO_3$, exhibited in Fig. 2, shows that the intensity ratio of the 003 and 104 peaks is quite high and exhibits a clear split of the (108) and (110) lines. The values of I_{003}/I_{104} for the $LiNi_{0.7}Co_{0.3}O_2$ and $LiCoO_2$ powders are 1.86 and 2.70, respectively, showing that the degree of displacement of the nickel and lithium ions is not high. They are much larger than that (0.87) for the $LiCoO_2$ from the JCPDS card #50–0653.

Fig. 3 shows SEM micrographs of $LiNi_{0.7}Co_{0.3}O_2$ synthesized at 800 °C using different combinations of starting materials: (a) Li_2CO_3, NiO, and $CoCO_3$, (b) $LiOH \cdot H_2O$, NiO, and Co_3O_4, (c) Li_2CO_3, NiO, and Co_3O_4, and (d) Li_2CO_3, $NiCO_3$, and $CoCO_3$. Particles of all the samples are very similar in microstructure; they have small particles and large particles with the surfaces of particles quite flat. Sample (c) exhibits the largest particles, followed in order by samples (d), (b), and (a).

The curves of voltage vs. x in $Li_xNi_{0.7}Co_{0.3}O_2$ at a current density of 200 μA/cm^2 for the first charge-discharge of $LiNi_{0.7}Co_{0.3}O_2$ synthesized at 800 °C using various

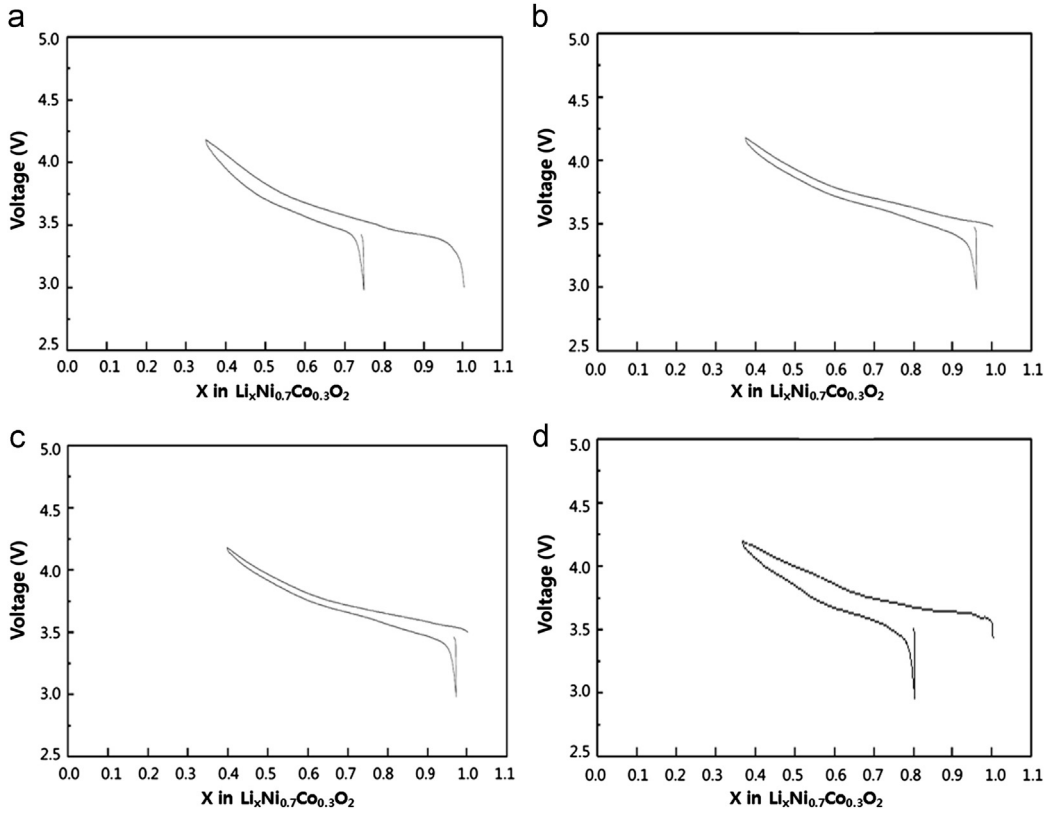

Fig. 4. Curves of voltage vs. x in $Li_xNi_{0.7}Co_{0.3}O_2$ at a current density of 200 μA/cm^2 for the first charge–discharge of $LiNi_{0.7}Co_{0.3}O_2$ synthesized at 800 °C using the following combinations of starting materials: (a) Li_2CO_3, NiO, and $CoCO_3$, (b) $LiOH \cdot H_2O$, NiO, and Co_3O_4, (c) Li_2CO_3, NiO, and Co_3O_4, and (d) Li_2CO_3, $NiCO_3$, and $CoCO_3$.

combinations of starting materials are shown in Fig. 4: (a) Li_2CO_3, NiO, and $CoCO_3$, (b) $LiOH \cdot H_2O$, NiO, and Co_3O_4, (c) Li_2CO_3, NiO, and Co_3O_4, and (d) Li_2CO_3, $NiCO_3$, and $CoCO_3$. Polarization represents a change in potentials for the deintercalation and intercalation of lithium atoms. Sample (c) exhibits the smallest polarization value, followed in order by samples (b), (a) and (d). Charge and discharge capacity are proportional to the value of Δx in $Li_xNi_{0.7}Co_{0.3}O_2$. The theoretical charge or discharge capacity is calculated by the following equation;

$$\text{the theoretical charge or dischargecapacity} = \frac{Fm\Delta x}{3600M}\ (\text{mAh/g}) \qquad (1)$$

where F is Faraday constant, m the weight of active material, and M the molecular weight of active material. The values of Δx in $Li_xNi_{0.7}Co_{0.3}O_2$ for discharge of the samples (b), (c), (d), and (a) are 0.59, 0.59, 0.44, and 0.40, respectively. The sample (b) has the largest discharge capacity (162 mAh/g), followed in order by sample (c) (158 mAh/g), sample (d) (133 mAh/g), and sample (a) (103 mAh/g).

Fig. 5 exhibits curves of voltage vs. x in $Li_xNi_{0.7}Co_{0.3}O_2$ for the first and second charge–discharge cycles for $LiNi_{0.7}Co_{0.3}O_2$ synthesized at 800 °C from Li_2CO_3, NiO, and Co_3O_4. The value of Δx for the second discharge is slightly smaller than that for the first discharge.

The variations of the discharge capacity with the number of cycles were investigated for two samples with relatively large

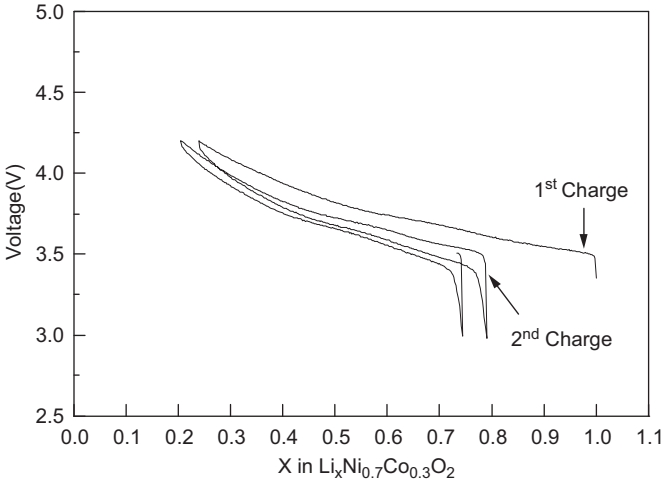

Fig. 5. Curves of voltage vs. x in $Li_xNi_{0.7}Co_{0.3}O_2$ for the first and second charge–discharge cycles for $LiNi_{0.7}Co_{0.3}O_2$ synthesized at 800 °C from Li_2CO_3, NiO, and Co_3O_4.

first discharge capacities, a sample synthesized from $LiOH \cdot H_2O$, NiO, and Co_3O_4, and a sample synthesized from Li_2CO_3, NiO, and Co_3O_4. A sample with the smallest first discharge capacity synthesized from Li_2CO_3, NiO, and Co_3O_4 was also examined. The variations of the discharge capacity with the number of cycles for $LiNi_{0.7}Co_{0.3}O_2$ synthesized at 800 °C from (a) Li_2CO_3, NiO, and Co_3O_4, (b) $LiOH \cdot H_2O$, NiO, and Co_3O_4, and

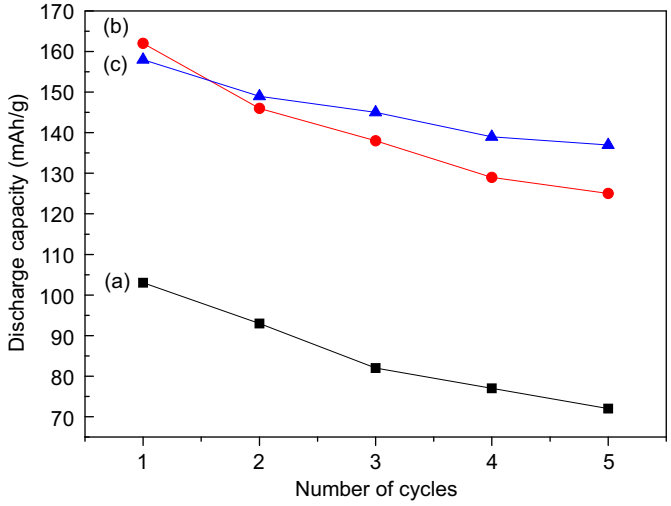

Fig. 6. Variations of the discharge capacity with the number of cycles for $LiNi_{0.7}Co_{0.3}O_2$ synthesized at 800 °C from (a) Li_2CO_3, NiO, and $CoCO_3$, (b) $LiOH \cdot H_2O$, NiO, and Co_3O_4, and (c) Li_2CO_3, NiO, and Co_3O_4.

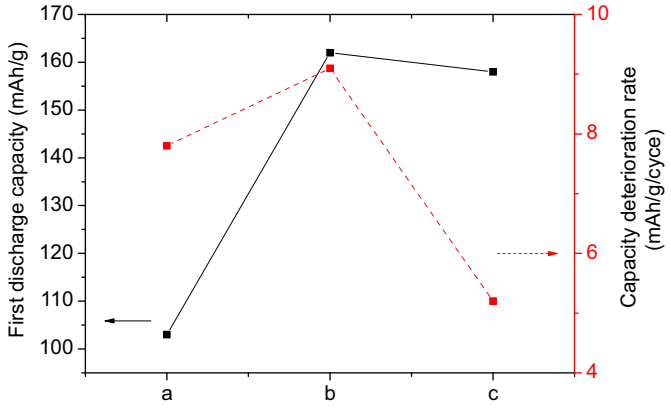

Fig. 7. Variations of the first discharge capacity and the capacity deterioration rate of the $LiNi_{0.7}Co_{0.3}O_2$ synthesized at 800 °C using the following combinations of starting materials: (a) Li_2CO_3, NiO, and $CoCO_3$, (b) $LiOH \cdot H_2O$, NiO, and Co_3O_4, and (c) Li_2CO_3, NiO, and Co_3O_4.

(c) Li_2CO_3, NiO, and Co_3O_4 are shown in Fig. 6. Sample (b) has the largest first discharge capacity (162 mAh/g), followed in order by samples (c) (158 mAh/g) and (a) (103 mAh/g). Sample (c) exhibits the best cycling performance, followed in order by samples (a) and (b). Kang et al. [43] previously investigated the structure and electrochemical properties of the $Li_xCo_yNi_{1-y}O_2$ ($y=0.1$, 0.3, 0.5, 0.7 and 1.0) system synthesized by solid-state reaction using various starting materials to optimize the characteristics and synthetic conditions of the $Li_xCo_yNi_{1-y}O_2$. They found that the first discharge capacities of $Li_xCo_yNi_{1-y}O_2$ were 60–180 mAh/g depending on synthesis conditions.

Fig. 7 shows the variations of the first discharge capacity and the capacity deterioration rate of $LiNi_{0.7}Co_{0.3}O_2$ synthesized at 800 °C using the following combinations of starting materials: (a) Li_2CO_3, NiO, and $CoCO_3$, (b) $LiOH \cdot H_2O$, NiO, and Co_3O_4, and (c) Li_2CO_3, NiO, and Co_3O_4. Sample (b) has the largest first discharge capacity, followed in order by samples (c) and (a). Sample (c) has the smallest capacity deterioration rate (5.2 mAh/g/cycle), followed in order by samples (a) (7.8 mAh/g/cycle), and (b) (9.1 mAh/g/cycle). The sample with the largest first discharge capacity has the largest capacity deterioration rate.

The curves of voltage vs. x in $Li_xNi_{0.7}Co_{0.3}O_2$ at a current density of 200 μA/cm^2 for the first charge–discharge of $LiNi_{0.7}Co_{0.3}O_2$ in Figs. 4 and 5 show that, compared with the quantity of the Li ions deintercalated by the first charging, that of the Li ions intercalated by the first discharging is much smaller. During the first charging, Li ions deintercalate not only from stable 3b sites but also from unstable 3b sites. The destruction of the unstable 3b sites, after deintercalation from unstable 3b sites, is thought to lead to much smaller quantity of the Li ions intercalated by the first discharging than that of the Li ions deintercalated by the first charging.

In the curves of voltage vs. x in $Li_xNi_{0.7}Co_{0.3}O_2$ at a current density of 200 μA/cm^2 for the first charge–discharge cycle shown in Fig. 4(b) and (c), and for the first and second charge–discharge cycles shown in Fig. 5 of $LiNi_{0.7}Co_{0.3}O_2$ synthesized at 800 °C from Li_2CO_3, NiO, and Co_3O_4, the charge–discharge curves exhibit quite long plateaus, where two phases co-exist [44]. During charging and discharging, $LiNiO_2$ goes reportedly through three or four phase transitions [39,45,46]. Song et al. [46] reported that–dx/|dV| vs. V curves of $LiNi_{1-y}Ti_yO_2$ ($y=0.012$ and 0.025) for charging and discharging showed four peaks, revealing four phase transitions from hexagonal structure (H1) to monoclinic structure (M), from M to hexagonal structure (H2), from H2 to hexagonal structure (H2) + hexagonal structure (H3), and from H2 + H3 to H3, or vice versa.

4. Conclusions

Cathode active materials with a composition of $LiNi_{0.7}Co_{0.3}O_2$ were synthesized by solid-state reaction at 800 °C using Li_2CO_3 or $LiOH \cdot H_2O$, NiO or $NiCO_3$, and $CoCO_3$ or Co_3O_4 as the sources of Li, Ni, and Co, respectively. The electrochemical properties of the synthesized samples were then investigated. A $LiNi_{0.7}Co_{0.3}O_2$ sample synthesized from $LiOH \cdot H_2O$, NiO, and Co_3O_4 exhibited the largest first discharge capacity of 162 mAh/g, with a discharge capacity deterioration rate of 9.1 mAh/g/cycle. The curves of voltage vs. x in $Li_xNi_{0.7}Co_{0.3}O_2$ for the first charge–discharge of $LiNi_{0.7}Co_{0.3}O_2$ showed that after deintercalation from unstable 3b sites, the unstable 3b sites would be destroyed, leading to a smaller quantity of the Li ions intercalated by the first discharging than that of the Li ions deintercalated by the first charging. The sample with the largest first discharge capacity had the largest capacity deterioration rate.

References

[1] K. Ozawa, Lithium-ion rechargeable batteries with $LiCoO_2$ and carbon electrodes: the $LiCoO_2$/C system, Solid State Ionics 69 (1994) 212–221.
[2] R. Alcántara, P. Lavela, J.L. Tirado, R. Stoyanova, E. Zhecheva, Structure and electrochemical properties of boron-doped $LiCoO_2$, Journal of Solid State Chemistry 134 (1997) 265–273.

[3] Z.S. Peng, C.R. Wan, C.Y. Jiang, Synthesis by sol–gel process and characterization of $LiCoO_2$ cathode materials, Journal of Power Sources 72 (1998) 215–220.

[4] W.D. Yang, C.Y. Hsieh, H.J. Chuang, Y.S. Chen, Preparation and characterization of nanometric-sized $LiCoO_2$ cathode materials for lithium batteries by a novel sol–gel method, Ceramics International 36 (1) (2010) 135–140.

[5] S.K. Kim, D.H. Yang, J.S. Sohn, Y.C. Jung, Resynthesis of $LiCo_{1-x}Mn_xO_2$ as a cathode material for lithium secondary batteries, Metals and Materials International 18 (2) (2012) 321–326.

[6] J.R. Dahn, U. von Sacken, C.A. Michal, Structure and electrochemistry of $Li_{1\pm y}NiO_2$ and a new Li_2NiO_2 phase with the $Ni(OH)_2$ structure, Solid State Ionics 44 (1990) 87–97.

[7] J.R. Dahn, U von Sacken, M.W. Juzkow, H. Al-Janaby, Rechargeable $LiNiO_2$/carbon cells, Journal of the Electrochemical Society 138 (1991) 2207–2212.

[8] B.H. Kim, J.H. Kim, I.H. Kwon, M.Y. Song, Electrochemical properties of $LiNiO_2$ cathode material synthesized by the emulsion method, Ceramics International 33 (2007) 837–841.

[9] H.U. Kim, D.R. Mumm, H.R. Park, M.Y. Song, Synthesis by a simple combustion method and electrochemical properties of $LiCo_{1/3}Ni_{1/3}Mn_{1/3}O_2$, Electronic Materials Letters 6 (3) (2010) 91–95.

[10] S.H. Ju, J.H. Kim, Y.C. Kang, Electrochemical properties of $LiNi_{0.8}Co_{0.2-x}Al_xO_2$ ($0 \le x \le 0.1$) cathode particles prepared by spray pyrolysis from the spray solutions with and without organic additives, Metals and Materials International 16 (2) (2010) 299–303.

[11] S.N. Kwon, J.H. Song, D.R. Mumm, Effects of cathode fabrication conditions and cycling on the electrochemical performance of $LiNiO_2$ synthesized by combustion and calcination, Ceramics International 37 (5) (2011) 1543–1548.

[12] M.Y. Song, C.K. Park, H.R. Park, D.R. Mumm, Variations in the electrochemical properties of metallic elements-substituted $LiNiO_2$ cathodes with preparation and cathode fabrication conditions, Electronic Materials Letters 8 (1) (2012) 37–42.

[13] M.Y. Song, D.R. Mumm, C.K. Park, H.R. Park, Cycling performances of $LiNi_{1-y}M_yO_2$ (M=Ni, Ga, Al and/or Ti) synthesized by wet milling and solid-state method, Metals and Materials International 18 (3) (2012) 465–472.

[14] J.M. Tarascon, E. Wang, F.K. Shokoohi, W.R. Mckinnon, S. Colson, The spinel phase of $LiMn_2O_4$ as a cathode in secondary lithium cells, Journal of the Electrochemical Society 138 (1991) 2859–2864.

[15] A.R. Armstrong, P.G. Bruce, Synthesis of layered $LiMnO_2$ as an electrode for rechargeable lithium batteries, Letters in Nature 381 (1996) 499–500.

[16] M.Y. Song, D.S. Ahn, On the capacity deterioration of Spinel phase $LiMn_2O_4$ with cycling around 4 V, Solid State Ionics 112 (1998) 21–24.

[17] M.Y. Song, D.S. Ahn, H.R. Park, Capacity fading of spinel phase $LiMn_2O_4$ with cycling, Journal of Power Sources 83 (1999) 57–60.

[18] D.S. Ahn, M.Y. Song, Variations of the electrochemica properties of $LiMn_2O_4$ with synthesis conditions, Journal of the Electrochemical Society 147 (3) (2000) 874–879.

[19] H.J. Guo, Q.H. Li, X.H. Li, Z.X. Wang, W.J. Peng, Novel synthesis of $LiMn_2O_4$ with large tap density by oxidation of manganese powder, Energy Conversion and Management 52 (4) (2011) 2009–2014.

[20] C. Wan, M. Cheng, D. Wu, Synthesis of spherical spinel $LiMn_2O_4$ with commercial manganese carbonate, Powder Technology 210 (1) (2011) 47–51.

[21] J.W. Park, J.H. Yu, K.W. Kim, H.S. Ryu, J.H. Ahn, C.S. Jin, K.H. Shin, Y.C. Kim, H.J. Ahn, Surface morphology changes of lithium/sulfur battery using multi-walled carbon nanotube added sulfur electrode during cyclings, Korean Journal of Metals and Materials 49 (2) (2011) 174–179.

[22] Y. Nishida, K. Nakane, T. Satoh, Synthesis and properties of Gallium-doped $LiNiO_2$ as the cathode material for lithium secondary batteries, Journal of Power Sources 68 (1997) 561–564.

[23] P. Barboux, J.M. Tarascon, F.K. Shokoohi, The use of acetates as precursors for the low-temperature synthesis of $LiMn_2O_4$ and $LiCoO_2$ intercalation compounds, Journal of Solid State Chemistry 94 (1991) 185–196.

[24] J. Morales, C. Perez-Vicente, J.L. Tirado, Cation distribution and chemical deintercalation of $Li_{1-x}Ni_{1+x}O_2$, Materials Research Bulletin 25 (1990) 623–630.

[25] B.J. Neudecker, R.A. Zuhr, B.S. Kwak, J.B. Bates, J.D. Robertson, Lithium manganese nickel oxides $Li_x(Mn_yNi_{1-y})_{2-x}O_2$, Journal of the Electrochemical Society 145 (1998) 4148–4157.

[26] A. Rougier, I. Saadoune, P. Gravereau, P. Willmann, C. Delmas, Effect of cobalt substitution on cationic distribution in $LiNi_{1-y}Co_yO_2$ electrode materials, Solid State Ionics 90 (1996) 83–90.

[27] C. Delmas, I. Saadoune, Electrochemical and physical properties of the $Li_xNi_{1-y}Co_yO_2$ phases, Solid State Ionics 53–56 (1992) 370–375.

[28] E. Zhecheva, R. Stoyanova, Stabilization of the layered crystal structure of $LiNiO_2$ by Co-substitution, Solid State Ionics 66 (1993) 143–149.

[29] C. Delmas, I. Saadoune, A. Rougier, The cycling properties of the $Li_xNi_{1-y}Co_yO_2$ electrode, Journal of Power Sources 43–44 (1993) 595–602.

[30] A. Ueda, T. Ohzuku, Solid-state redox reactions of $LiNi_{1/2}Co_{1/2}O_2$ ($R\bar{3}m$) for 4 V secondary lithium cells, Journal of the Electrochemical Society 141 (1994) 2010–2014.

[31] M. Menetrier, A. Rougier, C. Delmas, Cobalt segregation in the $LiNi_{1-y}Co_yO_2$ solid solution: a preliminary ^7Li NMR study, Solid State Commun 90 (1994) 439–442.

[32] R. Alcantara, J. Morales, J.L. Tirado, R. Stoyanova, E. Zhecheva, Structure and electrochemical properties of $Li_{1-x}(Ni_yCo_{1-y})_{1+x}O_2$ Effect of chemical delithiation at 0 °C, Journal of the Electrochemical Society 142 (1995) 3997–4005.

[33] B. Banov, J. Bourilkov, M. Mladenov, Cobalt stabilized layered lithium–nickel oxides, cathodes in lithium rechargeable cells, Journal of Power Sources 54 (1995) 268–270.

[34] Y.M. Choi, S.I. Pyun, S.I. Moon, Effects of cation mixing on the electrochemical lithium intercalation reaction into porous $Li_{1-\delta}Ni_{1-y}Co_yO_2$ electrodes, Solid State Ionics 89 (1996) 43–52.

[35] S.J. Lee, J.K. Lee, D.W. Kim, H.K. Baik, S.M. Lee, Fabrication of thin film $LiCo_{0.5}Ni_{0.5}O_2$ cathode for Li rechargeable microbattery, Journal of the Electrochemical Society 143 (1996) L268–L270.

[36] D. Caurant, N. Baffier, B. Garcia, J.P. Pereira-Ramos, Synthesis by a soft chemistry route and characterization of $LiNi_xCo_{1-x}O_2$ ($0 \le x \le 1$) cathode materials, Solid State Ionics 91 (1996) 45–54.

[37] K. Amine, H. Yasuda, Y. Fujita, New process for low temperature preparation of $LiNi_{1-x}Co_xO_2$ Cathode material for lithium cells, Annales de Chimie -*Science* des Matériaux 23 (1998) 37–42.

[38] C.C. Chang, N. Scarr, P.N. Kumta, Synthesis and electrochemical characterization of $LiMO_2$ (M=Ni, $Ni_{0.75}Co_{0.25}$) for rechargeable lithium ion batteries, Solid State Ionics 112 (1998) 329–344.

[39] T. Ohzuku, A. Ueda, M. Nagayama, Electrochemistry and structural chemistry of $LiNiO_2$ ($R\bar{3}m$) for 4 V secondary lithium cells, Journal of the Electrochemical Society 140 (1993) 1862–1870.

[40] M.Y. Song, H. Rim, E. Bang, Electrochemical properties of cathode materials $LiNi_{1-y}Co_yO_2$ synthesized using various starting materials, Journal of Applied Electrochemistry 34 (2004) 383–389.

[41] H. Rim, H.R. Park, M.Y. Song, Synthesis of lithium $LiNi_{1-y}Co_yO_2$ from lithium carbonate, nickel oxide and cobalt carbonate and their electrochemical properties, Ceramics International 38 (2012) 5987–5991.

[42] H. Rim, H.R. Park, M.Y. Song, Electrochemical performance of cobalt-substituted lithium nickel oxides synthesized from lithium and nickel carbonates and cobalt oxide, Ceramics International 39 (2013) 917–923.

[43] S.G. Kang, K.S. Ryu, S.H. Chang, S.C. Park, The novel synthetic route to $LiCo_yNi_{1-y}O_2$ as a cathode material in lithium secondary batteries, Bulletin of the Korean Chemical Society 22 (12) (2001) 1328–1332.

[44] W. Li, J.N. Reimers, J.R. Dahn, In situ X-ray diffraction and electrochemical studies of $Li_{1-x}NiO_2$, Solid State Ionics 67 (1993) 123–130.

[45] H. Arai, S. Okada, H. Ohtsuka, M. Ichimura, J. Yamaki, Characterization and cathode performance of $Li_{1-x}Ni_{1+x}O_2$ prepared with the excess lithium method, Solid State Ionics 80 (1995) 261–269.

[46] M.Y. Song, D.S. Lee, H.R. Park, Electrochemical properties of $LiNi_{1-y}Ti_yO_2$ and $LiNi_{0.975}M_{0.025}O_2$ (M=Zn, Al, and Ti) synthesized by the solid-state reaction method, Materials Research Bulletin 47 (2012) 1021–1027.